Structural Durability & Health Monitoring

Tech Science Press

Doi:10.32604/sdhm.2025.074148

ARTICLE

# A Robust Damage Identification Method Based on Modified Holistic Swarm Optimization Algorithm and Hybrid Objective Function

**Xiansong Xie**[1,*] **and Xiaoqian Qian**[2]

[1]School of Architectural Engineering, Quzhou University, Quzhou, 324000, China
[2]College of Civil Engineering and Architecture, Zhejiang University, Hangzhou, 310058, China

*Corresponding Author: Xiansong Xie. Email: lt2957327761@gmail.com

Received: 03 October 2025; Accepted: 13 November 2025; Published: 31 March 2026

**ABSTRACT:** Correlation function of acceleration responses-based damage identification methods has been developed and employed, while they still face the difficulty in identifying local or minor structural damages. To deal with this issue, a robust structural damage identification method is developed, integrating a modified holistic swarm optimization (MHSO) algorithm with a hybrid objective function. The MHSO is developed by combining Hammersley sequence-based population initialization, chaotic search around the worst solution, and Hooke-Jeeves pattern search around the best solution, thereby improving both global exploration and local exploitation capabilities. A hybrid objective function is constructed by merging acceleration correlation function-based and strain correlation function-based objective functions, effectively leveraging the complementary sensitivities of global and local responses. To further suppress spurious solutions and promote sparsity in parameter estimation, an additional $L_{0.5}$ regularization term is introduced. The effectiveness of the proposed method is validated through numerical simulations on a simply supported beam and a steel girder benchmark structure. Comparative studies with sequential quadratic programming, genetic algorithm, and HSO demonstrate that the MHSO achieves superior accuracy and convergence efficiency, even with limited sensors and 20% noise-contaminated measurements. Results highlight that the hybrid objective function significantly enhances the detection of both major and minor damages, while the inclusion of sparse regularization improves robustness against noise and model uncertainties. The findings indicate that the proposed framework provides a reliable and computationally efficient solution for simultaneous localization and quantification of structural damages, offering promising applicability to real-world structural health monitoring scenarios.

**KEYWORDS:** Damage identification; holistic swarm optimization algorithm; combined correlation function; hybrid objective function; sparse regularization; grid structure

## 1 Introduction

Ensuring the safety of civil infrastructure is a critical challenge, as bridges, towers, and other large-scale systems are continuously exposed to environmental and operational stresses [1]. Even minor damage, if left undetected, can propagate and lead to severe performance degradation or sudden collapse. Consequently, structural health monitoring (SHM) and damage identification have attracted significant research attention as indispensable tools for maintaining resilience and reducing life-cycle costs. The integration of advanced sensing technologies and artificial intelligence provides new opportunities to detect early-stage damage with high accuracy.

Current damage identification approaches can be broadly categorized into physics-based and data-driven methods. Physics-based approaches rely on structural models and inverse analysis, such as finite element model updating and vibration-based identification. On the other hand, data-driven approaches exploit sensor data and learning algorithms to directly map structural responses to damage patterns. Recent advances in machine learning and deep neural networks have significantly improved detection accuracy, even under noisy or incomplete data conditions. Among these methods, vibration-based techniques have emerged as one of the most widely adopted strategies for structural damage identification, primarily because vibration responses inherently capture global information about the system [2]. Frequency-domain methods rely on shifts in natural frequencies [3], mode shapes [4], modal strain energy [5], flexibility matrices [6], and frequency response functions [7], etc., to infer damage. These methods are attractive due to their simplicity, low computational requirements, and the ability to capture global damage signatures. Although these approaches have demonstrated high accuracy in many applications, their practical utility is limited by the insensitivity of low-order modes to minor damage and the difficulty of accurately extracting higher-order modes from real structures due to measurement noise [8].

In contrast to frequency-domain techniques, time-domain methods exploit detailed temporal responses such as acceleration or displacement signals. By incorporating techniques like impulse response analysis, autoregressive modeling, or time-series reconstruction, these methods provide richer information for identifying both the location and severity of damage. Their major strength lies in sensitivity to local changes, but they are more vulnerable to measurement noise and require higher data quality. Several representative approaches have been developed and successfully applied, including the iterative least squares method [9], maximum likelihood estimation [10], extended Kalman filter [11], and particle filter [12]. These classical methods are grounded in rigorous mathematical theory and offer reliable frameworks for parameter estimation. However, their effectiveness strongly depends on providing accurate initial guesses of the unknown parameters and on the availability of appropriate gradient information. Moreover, their inherent point-to-point search mechanism increases the risk of premature convergence, making them prone to being trapped in local optima, particularly when dealing with highly nonlinear or large-scale structural systems.

In recent years, machine learning techniques, particularly neural networks and heuristic optimization algorithms, have emerged as powerful tools for structural damage identification [13,14]. Neural networks excel at learning hidden patterns from large datasets, enabling automated feature extraction and damage classification. Meanwhile, heuristic optimization algorithms provide efficient search capabilities in high-dimensional spaces, making them well-suited for solving inverse identification problems [15]. Genetic algorithm (GA) [16], differential evolution (DE) [17], artificial bee colony algorithm [18], tree seeds algorithm [19], monkey algorithm [20], gray wolf optimization [21], exponential-trigonometric optimization algorithm [22], improved termite life cycle optimizer [23], and slime mold algorithm [24], have been adopted due to their simplicity, flexibility, and robustness. For instance, Zhou et al. [25] introduced an improved butterfly optimization algorithm that integrates a sampling technique and search space reduction method to enhance structural parameter identification. Xu et al. [26] combined particle swarm optimization (PSO) with support vector machines to determine the damage extent of carbon fiber reinforced polymer cables. These studies indicate that computational intelligence approaches exhibit strong potential and effectiveness. Nevertheless, they still encounter the following three challenges:

First, for most heuristic algorithms, to determine algorithm-specific parameters, trial-and-error procedures not only demand considerable computational resources but also undermine their applicability in large-scale problems. Second, structural excitations such as wind or traffic loads are often unavailable in real engineering environments, highlighting the need for output-only identification methods that can operate under unknown ambient excitations. Third, practical issues including high levels of measurement noise,

minor or localized damage, and limited sensor availability are rarely addressed in existing studies, yet they frequently occur in real-world applications. These challenges underscore the necessity of developing more robust, adaptive, and practically oriented approaches for structural damage identification.

To address the first challenge, notable progress has been made in metaheuristic optimization. Recent years have witnessed the rapid proliferation of algorithms inspired by natural, physical, and social metaphors. Although such approaches have demonstrated competitive performance, increasing evidence suggests that metaphorical analogies are not essential for designing efficient optimizers. Instead, more rigorous and generalizable frameworks can be developed without reliance on metaphors. Within this paradigm, the Holistic Swarm Optimization (HSO) algorithm [27] has been proposed as a novel metaphorless framework that utilizes information from the entire population to guide the search process. In contrast to existing metaphorless optimizers such as Jaya [28] and the Rao family of algorithms [29], which rely on best-worst interactions or limited statistical comparisons, HSO systematically integrates feedback from the global population distribution to determine search directions. Nevertheless, HSO often suffers from slow convergence and premature stagnation, which can largely be attributed to its relatively simplistic updating mechanism and insufficient adaptability in balancing global exploration with local exploitation. To overcome these limitations, this study introduces a modified HSO (MHSO) by integrating advanced strategies, including Hammersley sequence-based population initialization, chaotic search around the worst solution, and Hooke-Jeeves pattern search around the best solution, thereby enhancing both exploration and exploitation capabilities.

To address the second challenge, some output-only damage identification approaches have been proposed. Ni et al. [30] introduced a method based on the correlation functions of acceleration responses, which successfully identified damages in a laboratory four-story steel frame. Wang et al. [31] further extended the correlation functions by incorporating four different evolutionary algorithms and validated their effectiveness on the ASCE benchmark frame structure. To mitigate the potential influence of improper reference point selection, Zhang et al. [32] developed an adjacent acceleration correlation function approach, yielding satisfactory identification accuracy. However, structural damage is inherently a localized phenomenon [33]. Strain-based measurements can offer higher sensitivity to local variations, enabling the detection of small-scale damage. For instance, Li et al. [34] proposed a strain covariance response function method, demonstrating its ability to detect damage under white noise excitation. Similarly, Li et al. [35] utilized the amplitude vector of dynamic strain cross-correlation functions to detect structural damage. Nevertheless, a large number of strain gauges are typically required.

To address the last challenge, the use of multiple types of sensors has been increasingly advocated due to their complementary characteristics. Accelerometers provide global structural responses, while strain gauges are capable of capturing localized damage information. By integrating local and global measurements, the limitations of single-sensor approaches can be alleviated, leading to more accurate and reliable identification results. For instance, accelerometers and strain gauges have been jointly applied for structural damage detection [36], foundation system parameters estimation [37], random excitations reconstruction [38], and detection cracks as well as bolt loosening in steel frames [39]. In practical applications, damages in the Tsing Ma suspension bridge were successfully identified with the aid of a multi-sensor monitoring system [40].

This study presents a novel approach for structural damage identification that integrates a modified holistic swarm optimization algorithm with a hybrid objective function. The proposed MHSO enhances the traditional HSO by introducing three key strategies: Hammersley sequence-based population initialization to ensure uniform search space coverage, chaotic search mechanisms around the worst solution to enhance exploration, and Hooke-Jeeves pattern search around the best solution to accelerate convergence and

improve local exploitation. Simultaneously, a hybrid objective function is formulated by combining acceleration correlation functions with strain correlation functions, leveraging their complementary sensitivities to damage. This hybrid formulation enhances the detection of small or localized damages while maintaining robustness against noise, and significantly reduces the number of required sensors compared to strain-only approaches. To further improve performance in sparse damage scenarios, the $L_{0.5}$ sparse regularization technique [41] is incorporated. For validation, four objective functions are compared alongside sequential quadratic programming [42], genetic algorithm, and HSO. Numerical case studies on a simply-supported beam and a steel girder benchmark structure demonstrate that the proposed MHSO with hybrid objective function achieves superior performance in both damage localization and severity quantification, offering a promising tool for practical structural health monitoring applications.

## 2 Combined Correlation Function-Based Damage Identification

### *2.1 Structural Damage Identification Problem*

Optimization-based structural damage identification treats damage detection as an inverse problem, aiming to infer unknown damage parameters by minimizing the difference between experimentally measured and numerically predicted structural responses. The underlying principle is that damage induces changes in structural properties, which alter the dynamic behavior of the system. By systematically comparing measured vibration responses with computational model outputs, both the location and severity of damages can be accurately estimated.

The identification process generally begins with establishing a high-fidelity finite element model of the intact structure. Structural damage is generally modeled as a reduction in stiffness [43,44]. A damage model is then introduced to simulate local deterioration, where $\alpha_i$ is the damage index representing the stiffness reduction of the $i$-th element. An objective function is constructed to quantify the discrepancy between measured and reconstructed responses, serving as the criterion for damage identification. Optimization algorithms, including genetic algorithms, particle swarm optimization, differential evolution, and hybrid swarm strategies, iteratively adjust the damage indices to minimize this objective function.

### *2.2 Hybrid Objective Function*

Correlation functions of acceleration have been widely applied in structural damage identification due to their ability to capture dynamic relationships between different measurement points without requiring explicit input force information. These functions are effective in detecting large-scale damages by highlighting changes in vibration patterns. Their main advantages include robustness to noise and simplicity of implementation [30–32]. In Ref. [45], the combined correlation function of acceleration responses was proposed, which eliminates the need for selecting reference points, enhancing robustness and improving damage localization accuracy, especially in complex structural systems.

$$R_{\ddot{u}} = \left[R_{\ddot{u}_{1,2}}, R_{\ddot{u}_{1,3}}, \ldots, R_{\ddot{u}_{1,na}}, R_{\ddot{u}_{2,3}} \ldots, R_{\ddot{u}_{2,na}}, R_{\ddot{u}_{3,4}} \ldots, R_{\ddot{u}_{na-1,na}}\right]^T \tag{1}$$

where $na$ denotes the total number of accelerometers.

The objective function based on the combined correlation function of acceleration response, denoted as $Obj1$, is defined as

$$Obj1 = \sum_{i=1}^{na} \sum_{j=1}^{np} \frac{\left|R_{mea}(i,j) - R_{est}(i,j)\right|^2}{E\left({R_{mea}}^2(i)\right)} \tag{2}$$

where $R_{mea}$ and $R_{est}$ are the combined correlation function of the measured and estimated acceleration response, respectively; *na* and *np* are the number of measurements and data points; $E\left({R_{mea}}^2(i)\right) = \sum_{n=1}^{np} {R_{mea}}^2(i,\ j)/np$ stands for the mean squared value of the *i*-th measured combined correlation function.

Similarity, combined correlation function of strain responses is given as

$$\widehat{R}_{\varepsilon} = \left[\widehat{R}_{\varepsilon_{1,2}}, \widehat{R}_{\varepsilon_{1,3}}, \ldots, \widehat{R}_{\varepsilon_{1,ns}}, \widehat{R}_{\varepsilon_{2,3}} \ldots, \widehat{R}_{\varepsilon_{2,ns}}, \widehat{R}_{\varepsilon_{3,4}} \ldots, \widehat{R}_{\varepsilon_{ns-1,ns}}\right]^T \tag{3}$$

where *ns* represents the number of strain gauges.

The objective function based on the combined correlation function of strain response, denoted as *Obj*2, is defined as

$$Obj2 = \sum_{i=1}^{ns}\sum_{j=1}^{np} \frac{\left|\widehat{R}_{mea}(i,j) - \widehat{R}_{est}(i,j)\right|^2}{E\left({\widehat{R}_{mea}}^2(i)\right)} \tag{4}$$

where $\widehat{R}_{mea}$ and $\widehat{R}_{est}$ are the combined correlation function of the measured and estimated strain responses; *ns* and *np* mean the number of measurements and data points.

Simultaneously using acceleration and strain measurements for structural damage identification provides a more comprehensive and reliable assessment of structural health. Acceleration sensors capture global dynamic responses, reflecting overall structural behavior and enabling detection of major damage. However, they are often insensitive to minor or localized damages, as such changes may not significantly affect global vibration characteristics. Strain sensors, in contrast, are highly sensitive to local deformations and can detect subtle damage at specific locations. Their limitation lies in the fact that they provide only localized information, requiring dense sensor deployment for full coverage, which increases cost and complexity. By combining acceleration and strain data, these complementary strengths are leveraged. Acceleration offers global insight while strain provides fine-grained local detection. This integrated approach enhances damage detection accuracy, reduces false negatives, and improves robustness against noise, making it highly effective for practical structural health monitoring applications where both local and global damage information is essential. Moreover, simultaneous use of multiple types of sensors is more consistent with the actual situation of structural health monitoring. Therefore, a novel objective function, denoted as *Obj*3, is established using the combined acceleration correlation function-based objective function *Obj*1 and combined strain correlation function-based objective function *Obj*2 as follows

$$Obj3 = \Delta_1 \cdot Obj1 + \Delta_2 \cdot Obj2 \tag{5}$$

where $\Delta_1$ and $\Delta_2$ stand for the weight coefficients. They are introduced into the objective function to balance the *Obj*1 and *Obj*2 according to their sensitivity to elemental damages, and they can be calculated as

$$\Delta_1 = \frac{\sum_{j}^{ne}\sum_{i}^{nd}\left(Obj1_{ij}\right)/\left(Obj2_{ij}\right)}{\sum_{j}^{ne}\sum_{i}^{nd}\left(Obj1_{ij}\right)/\left(Obj2_{ij}\right) + ne^2},\ \Delta_2 = 1 - \Delta_1 \tag{6}$$

where $Obj1_{ij}$ and $Obj2_{ij}$ mean the value of $Obj1$ and $Obj2$ for the $i$-th damage level of the $j$-element; $ne$ and $nd$ stand for the number of elements and damage levels. Ten damage levels, i.e., $nd = \{0.1, 0.2, 0.3, 0.4, 0.5, 0.6, 0.7, 0.8, 0.9, 1.0\}$ are considered.

Incorporating a sparsity term into the objective function enhances structural damage identification by promoting sparse solutions, reflecting the realistic scenario that damages are usually localized. This regularization reduces ill-conditioning in the inverse problem, improves identification accuracy, and suppresses noise effects, enabling more precise localization and quantification of damage with fewer false positives. The new objective function based on $Obj3$ and sparse regularization, denoted as $Obj4$, is presented in following equation

$$Obj4 = \Delta_1 \cdot Obj1 + \Delta_2 \cdot Obj2 + \lambda \left\| \alpha \right\|_{0.5} \tag{7}$$

where $\lambda$ denotes the regularization parameter; $\left\| \alpha \right\|_{0.5}$ represents the $L_{0.5}$ norm of the solution.

Compared with the $L_1$ and $L_2$ regularization, the $L_{0.5}$ regularization is more suitable to stimulate the sparsity of structural damages. Introducing the sparse penalty item $\lambda \left\| \alpha \right\|_{0.5}$ can refine the ill-condition of the original problem and improve robustness to noise. The effectiveness of the proposed four objective functions, i.e., $Obj1$, $Obj2$, $Obj3$, $Obj4$, will be verified and compared in the present study.

## 3 Identification Algorithms

### *3.1 Basic Holistic Swarm Optimization Algorithm*

The Holistic Swarm Optimization (HSO) algorithm [27], proposed by Akbari in 2025, is an advanced metaheuristic optimization method inspired by swarm intelligence. Unlike traditional heuristic algorithms such as GA, PSO, DE, Jaya algorithm, Artificial bee colony (ABC) algorithm, which often depend on partial or pairwise information, HSO could dynamically balance exploration and exploitation using whole population information in iteration process. Specifically, the algorithm defines displacement coefficients using the root-mean-squared (RMS) fitness values of the population, ensuring that agents are systematically attracted toward promising regions and repelled from poor solutions. This mechanism provides a global, population-level perspective that significantly enhances search efficiency and robustness compared to local or sample-based strategies. A brief review of the proposed HSO algorithm is described as follows:

The initialization of the population is performed by generating individuals randomly within the upper limit $U_{i,j}$ and lower $L_{i,j}$. Mathematically, the initialization can be expressed as

$$X_{i,j} = L_{i,j} + rand\,(0,1) \times \left(U_{i,j} - L_{i,j}\right) \tag{8}$$

where $X_{i,j}$ denotes the value of the $j$-th variable for the $i$-th candidate in the population; $rand(0, 1)$ stands for a uniformly distributed random number between 0 and 1; In Eq. (8), $i \in (1, 2, \ldots, NP)$, $j \in (1, 2, \ldots, Dim)$, population size $NP$ and the dimension $Dim$ define the total number of individuals and the number of variables to be optimized.

Each individual represents a candidate solution for the optimized problem. The fitness of each individual is calculated. Then, the whole-population information is considered by using root-mean-squared (RMS) fitness values as follows

$$RMS_f = \sqrt{\frac{1}{n}\sum_{1}^{n} f\left(X_i\right)^2} \tag{9}$$

where $f\left(X_i\right)$ means the fitness value of the $i$-th agent.

The difference between the *RMS* and fitness value of the $i$-th agent is computed by

$$d_i = RMS_f - f(X_i) \tag{10}$$

Next, calculate the displacement coefficients. The coefficients $c_i$ are set positive or negative depending on whether the difference is below or above the *RMS*, and then normalized so that their absolute sum equals one

$$c_i = \frac{sign(d_i) \cdot |d_i|}{\sum_{i=1}^{n} |d_i|} \tag{11}$$

where $sign(d_i)$ stands for the *sign* function.

The positions of the search agents are updated in an iterative manner. At each iteration, the position of an agent $X_i$ is adjusted based on a weighted combination of the differences between its current position and the positions of the remaining agents in the population. The corresponding position-update formulation can be expressed as

$$X_i' = X_i + \chi \sum_{j=1}^{n} \gamma_{ij} \cdot c_j \cdot (X_j - X_i) \tag{12}$$

where $\chi$ is a fixed parameter, and $\gamma_{ij}$ is a random factor that introduces diversity and ensures a more exhaustive search of the solution space.

The flowchart of the basic holistic swarm optimization algorithm is shown in Fig. 1.

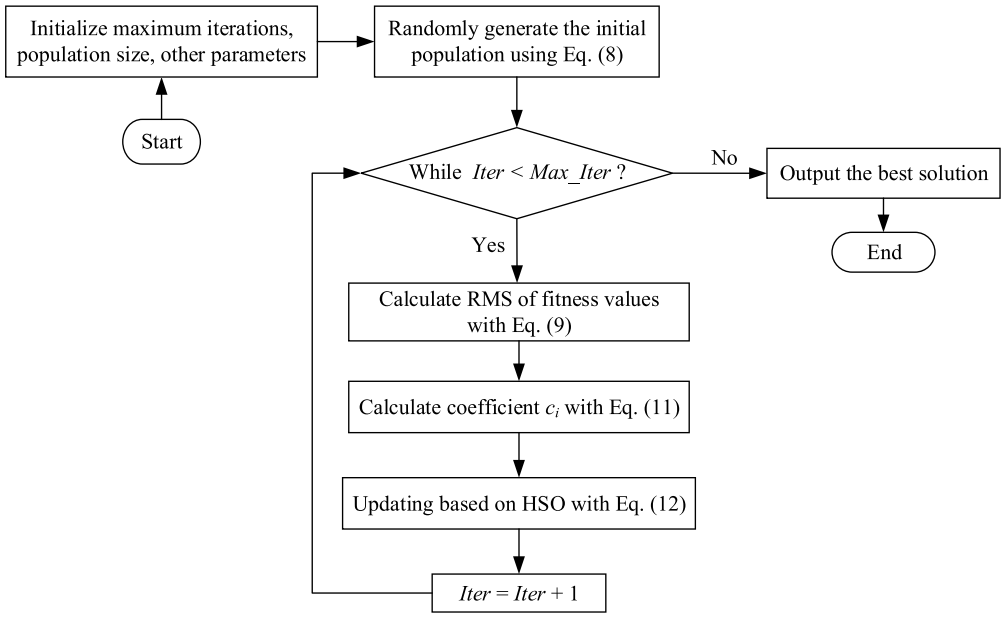


**Figure 1:** The flowchart of the basic holistic swarm optimization algorithm

### *3.2 Modified Holistic Swarm Optimization Algorithm*

To enhance the efficiency and robustness of the basic HSO algorithm, a modified variant is developed by incorporating three strategies in this section including population initialization with Hammersley sequence, chaotic search around the worst solution, and Hooke–Jeeves pattern search around the best solution.

*3.2.1 Population Initialization with Hammersley Sequence*

Population initialization plays a critical role in the performance of swarm intelligence algorithms. Traditional random initialization in Eq. (8) often leads to uneven distribution of individuals, causing premature convergence or insufficient coverage of the search space. To overcome this limitation, the Hammersley sequence [46] can be employed to generate the initial population. The Hammersley sequence belongs to the family of low-discrepancy sequences, which are designed to uniformly distribute points in a multidimensional space. By using this quasi-random sequence, individuals are placed more evenly across the feasible domain, thereby ensuring a comprehensive sampling of the search space. This improves the algorithm's global search ability and reduces the risk of stagnation in local optima.

The implementation process is straightforward. First, the dimensionality of the optimization problem is determined. Then, the Hammersley sequence is generated according to the problem dimension and population size, producing uniformly distributed points within the unit hypercube. Finally, these points are mapped to the actual search domain by following equation.

$$X_{i,j} = L_{i,j} + \psi \times \left(U_{i,j} - L_{i,j}\right) \tag{13}$$

where $\psi$ means the Hammersley sequence with $NP$ rows and $Dim$ columns.

This initialization strategy provides the algorithm with a well-spread and diverse population, which enhances convergence speed and solution quality.

*3.2.2 Chaotic Search around the Worst Solution*

In the basic holistic swarm optimization algorithm, whole population information is used while the worst solution is not well considered. In fact, the worst solution in the population often provides limited contribution to the search process and may even hinder convergence due to its poor fitness and lack of exploration potential. Such inferior individuals tend to reduce the overall population diversity and accelerate premature convergence, particularly in complex, multimodal optimization landscapes. To mitigate this drawback, a chaotic search strategy is incorporated to adjust the worst solution dynamically. Specifically, the tent map [47] is employed to generate a chaotic sequence with superior ergodicity and uniformity compared to conventional random sequences. The tent mapping is defined as

$$X_{n+1} = \begin{cases} \zeta X_n, & 0 \le X_n \le 0.5 \\ \zeta\left(1 - X_n\right), & 0.5 < X_n \le 1 \end{cases} \tag{14}$$

where $\zeta = 2$ and $X_n \in [0,1]$.

By iterating tent map, a series of chaotic numbers is obtained and then linearly transformed into the feasible solution space. The reconstructed candidates generated from the chaotic sequence replace or perturb the worst solution, and the best-performing candidate is retained. This mechanism not only prevents the stagnation caused by the worst individual but also introduces adaptive randomness, thereby enhancing the global search capability and robustness of the algorithm.

*3.2.3 Hooke–Jeeves Pattern Search around the Best Solution*

In swarm intelligence algorithms, the best solution plays a dominant role in guiding the population toward promising regions of the search space. However, excessive dependence on the current best solution may lead to premature convergence, particularly when the best individual is trapped in a local optimum. To address this issue, the Hooke–Jeeves (HJ) pattern search method [48] is introduced to refine the best

solution through a systematic local exploration process. The HJ algorithm alternates between exploratory moves, which probe the neighborhood of the current best solution along coordinate directions, and pattern moves, which accelerate the search toward more promising regions based on successful exploratory steps. Exploratory moves and pattern moves are repeated until a termination criterion is met, as presented in Fig. 2.

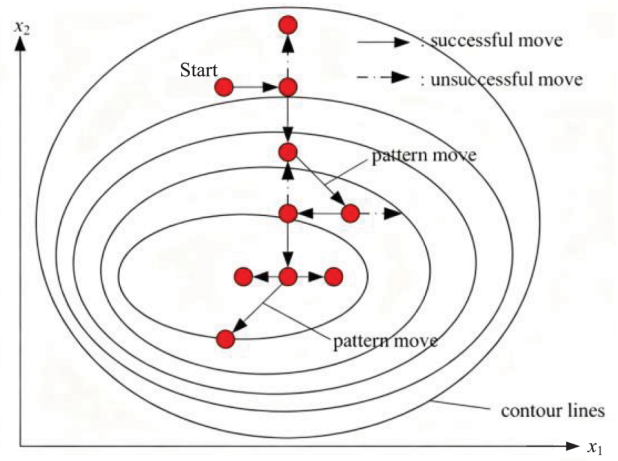


**Figure 2:** Hooke–Jeeves pattern search method

By embedding HJ pattern search into the optimization framework, the best solution is locally intensified and adaptively updated. This hybridization not only strengthens the exploitation ability of the algorithm but also improves convergence accuracy while maintaining computational efficiency. Consequently, the incorporation of the Hooke–Jeeves pattern search enhances the balance between exploration and exploitation, enabling the holistic swarm optimization algorithm to achieve more reliable performance in high-dimensional and multimodal optimization problems.

### *3.2.4 Framework of the Modified Holistic Swarm Optimization Algorithm*

Fig. 3 shows the flowchart of the proposed modified holistic swarm optimization (MHSO) algorithm. In the proposed MHSO, initial individuals are generated with Hammersley sequence across the feasible domain, thereby improving population diversity and providing a more representative sampling of the search space compared with purely random initialization. Then, all agents in the population are divided into common agent, the worst agent and the best agent. Different search operations are implemented corresponding to the type of agent. Specifically, common agents are updated using basic HSO. A tent mapping-based chaotic search is applied to the worst individual, enabling it to escape low-quality regions and explore new promising areas. An HJ pattern search is performed in the vicinity of the best solution, where exploratory and pattern moves accelerate progress toward high-quality optima. By seamlessly integrating these mechanisms into the HSO framework, the proposed MHSO algorithm achieves a better balance between exploration and exploitation, accelerates convergence, and enhances robustness in solving complex nonlinear and high-dimensional optimization problems.

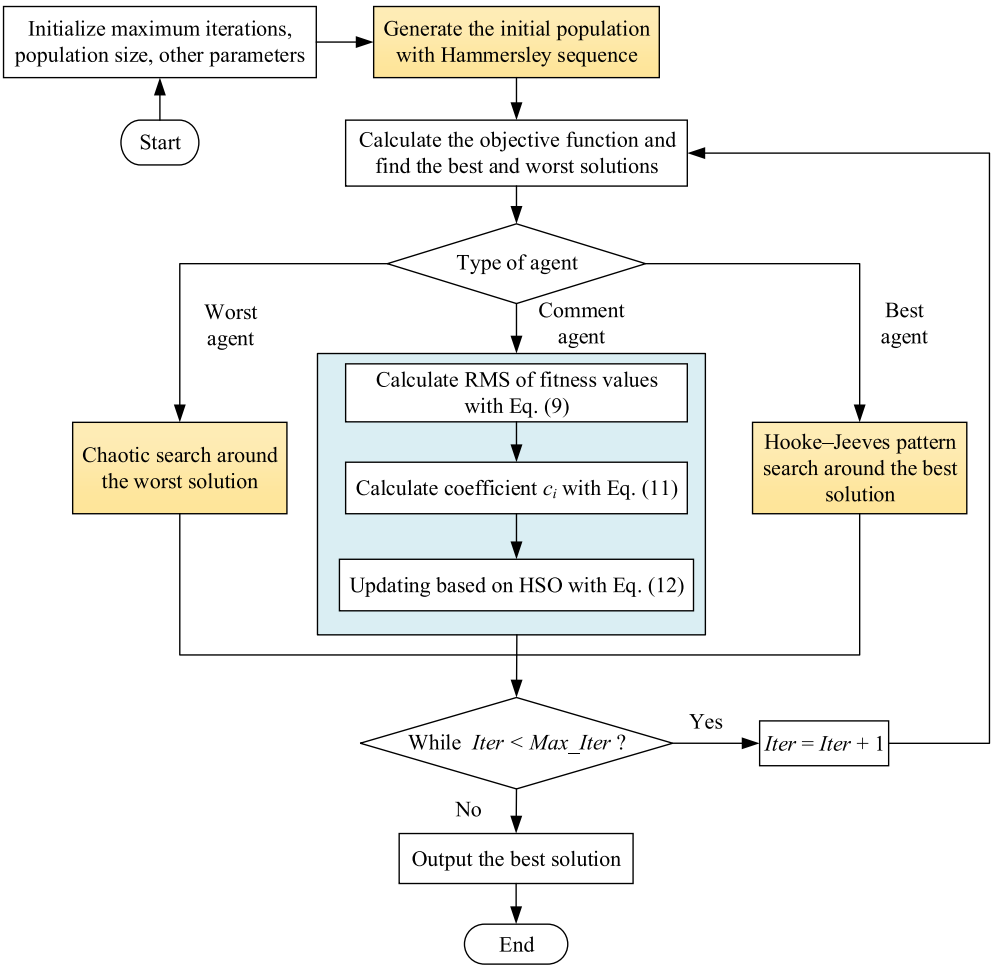


**Figure 3:** The flowchart of the proposed modified holistic swarm optimization algorithm

## 4 Procedures of Damage Identification

The implementation of the proposed output-only structural damage identification method, as shown in Fig. 4, integrating the MHSO algorithm with a hybrid objective function based on the combination of acceleration correlation function and strain correlation function involves the following key steps:

Step 1: Structural system is instrumented with a sparse network of acceleration and strain sensors to collect dynamic responses under ambient or operational loading.

Step 2: Compute combined acceleration correlation function $R_{mea}$ and combined strain correlation function $\widehat{R}_{mea}$ with the selected reference points.

Step 3: Initial finite element model of the target structure is constructed, and initial solutions $\theta_0$ for the optimization process are generated.

Step 4: Compute the estimated acceleration correlation function $R_{est}(\theta_i)$ and estimated strain correlation function $\widehat{R}_{est}(\theta_i)$. Evaluate the hybrid objective function using Eqs. (5) or (7) for each candidate solution $\theta_i$.

Step 5: MHSO algorithm iteratively minimizes the hybrid objective function by updating structural parameters.

Step 6: Repeat Step 3 to Step 5 until a predefined convergence criterion or maximum iteration count is reached.

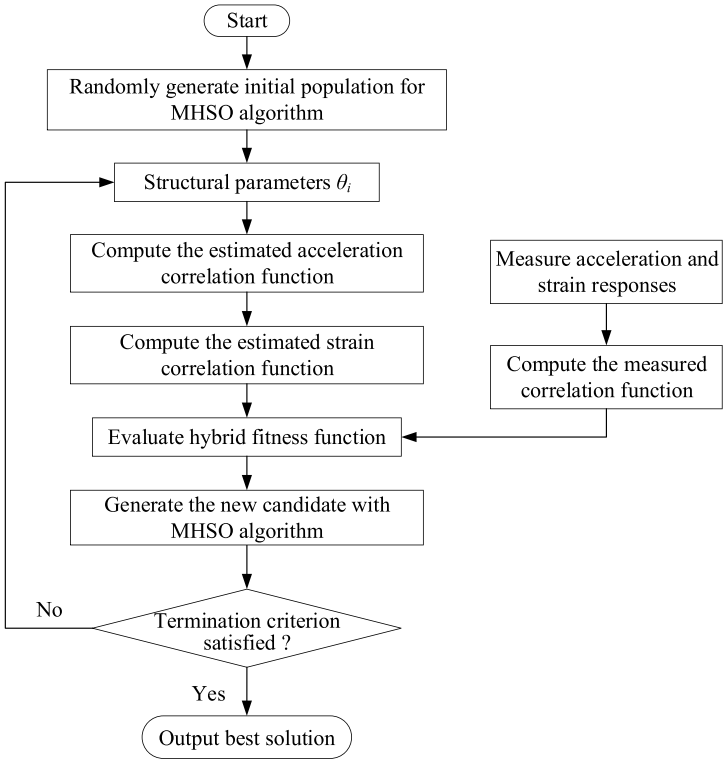


**Figure 4:** The flowchart of the proposed output-only structural damage identification method

## 5 Numerical Studies

To verify the feasibility and accuracy of the proposed method, a simply supported beam was employed as a test case. The finite element analysis is implemented using MATLAB R2021b on a Windows 10 64-bit platform, powered by an Intel Core i7-12700 CPU at 2.10 GHz with 32 GB of RAM. As show in Fig. 5, a detailed finite element model of the beam is constructed using beam elements with sufficiently refined discretization to ensure computational precision. The beam considered has a total length of 1.6 m, a width of 50 mm, and a height of 3 mm. The beam is discretized into 16 equal-length elements, resulting in 17 nodes with a nodal spacing of 100 mm. Each intermediate node is assigned two degrees of freedom. Boundary conditions are ideal simply supported constraints at both ends of the beam. Material properties, including Young's modulus and density are $E = 2.1 \times 10^{11}$ N/m$^2$ and $\rho = 7850$ kg/m$^3$, respectively.

Four damage cases and measurement arrangements on the simply-supported beam structure are studied, shown in Fig. 5 and Table 1. Structural simulated responses including acceleration and strain signals are recorded. These data sets are used as reference inputs to test the proposed method's performance in accurately identifying damage locations and quantifying damage severity. The simulation is conducted over a total duration of 1800 s, with a sampling frequency of 400 Hz to ensure high-resolution capture of the structural dynamic response. To comprehensively evaluate the capability of the proposed method, damage scenarios of varying severity are systematically investigated. Specifically, damage levels are classified into two categories: severe damage and minor damage. Severe damage is defined as cases where the damage extent exceeds 10% of the structural parameter under consideration, representing significant degradation of

structural integrity. Minor damage corresponds to situations in which the damage extent is equal to or below 10%, representing early-stage or subtle structural deterioration. This categorization allows for the assessment of the method's sensitivity and robustness across a wide range of damage conditions.

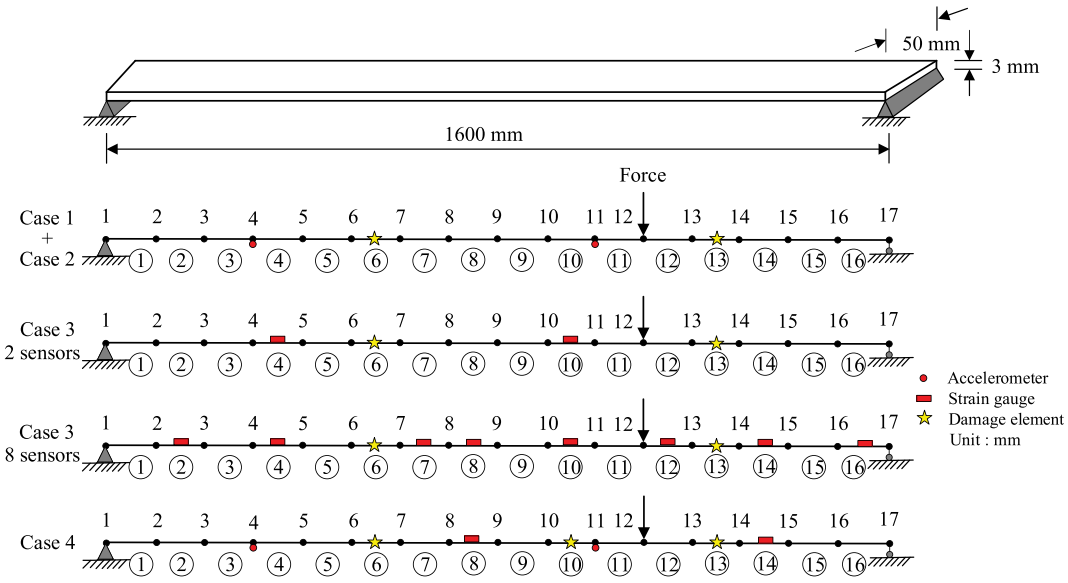


**Figure 5:** 16-element simply-supported beam structure

**Table 1:** Four different damage and measurement cases for a simply-supported beam

| Damage cases | Damage type | Data type | Objective function | Element no. | Damage extent |
|---|---|---|---|---|---|
| Case 1 | Large damages | Acceleration | *Obj*1 | 6, 13 | $\alpha_6 = 30\%$, $\alpha_{13} = 15\%$ |
| Case 2 | Small damages | Acceleration | *Obj*1 | 6, 13 | $\alpha_6 = 10\%$, $\alpha_{13} = 8\%$ |
| Case 3 | Small damages | Strain | *Obj*2 | 6, 13 | $\alpha_6 = 10\%$, $\alpha_{13} = 6\%$ |
| Case 4 | Large + small damages | Acceleration + strain | *Obj*3/*Obj*4 | 6, 10, 13 | $\alpha_6 = 20\%$, $\alpha_{10} = 10\%$, $\alpha_{13} = 6\%$ |

### *5.1 Comparison on Different Objective Functions*

Identification of structural damages using the proposed MHSO algorithm with four different objective functions, i.e., *Obj*1, *Obj*2, *Obj*3, *Obj*4, is performed and compared. Regarding the configuration of the proposed MHSO algorithm, key parameters are selected to balance computational efficiency and identification accuracy. The algorithm is executed with a population size of 100 agents and a maximum number of 200 iterations. To ensure the robustness of the identification results, the reported performance is based on the average results from 30 independent trials, minimizing the influence of random variations inherent to heuristic optimization. Furthermore, to assess the method's robustness, white Gaussian noise with noise levels of 0%, 10%, and 20% are considered. By incorporating these noise scenarios, the performance of the proposed method can be systematically tested under varying signal-to-noise ratios, thereby demonstrating its reliability and practical applicability in structural health monitoring under imperfect measurement conditions.

The combined correlation function of acceleration responses based objective function *Obj*1 is employed to identify both large and small structural damages. In damage case 1, stiffness reductions of 30% and 15% are introduced in elements 6 and 13, respectively. In damage case 2, smaller stiffness reductions of 10% and 8% are assumed in elements 6 and 13. For both cases, acceleration responses are extracted from nodes 4 and 11. The identification results obtained with *Obj*1 are illustrated in Fig. 6. In case 1, the large damages are successfully identified with a mean error of 1.75% and a maximum error of 7.69% under 20% measurement noise. In contrast, the locations and severities of the small damages in case 2 are not detected. These findings suggest that while the combined acceleration correlation function-based objective function is effective in identifying relatively large damages, it may not be sufficiently sensitive to capture small or minor damage scenarios.

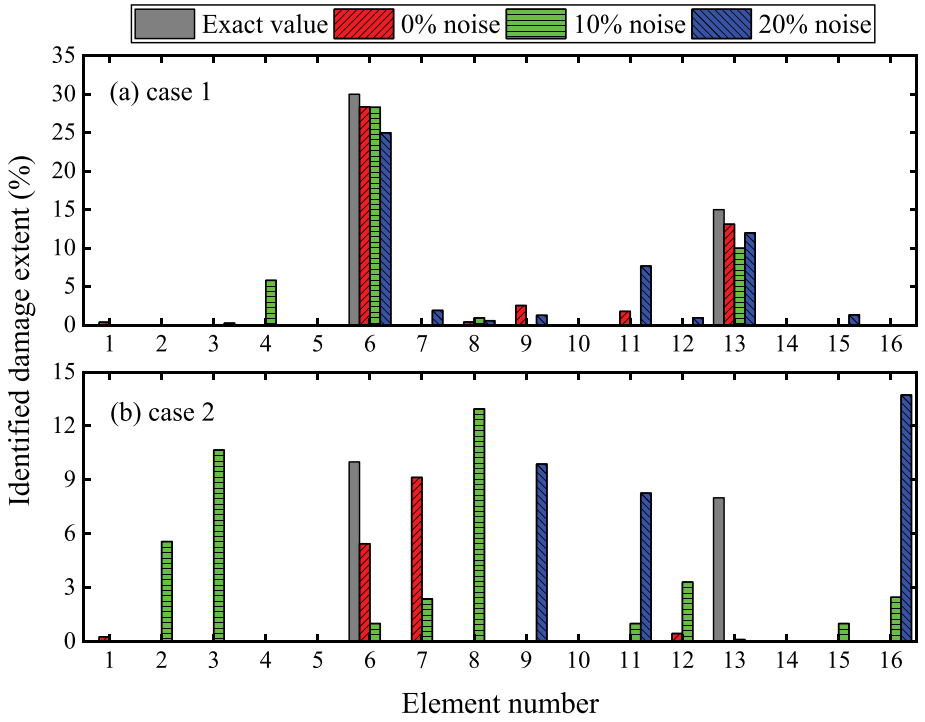


**Figure 6:** Damage identification with *Obj*1: (**a**) case 1; (**b**) case 2

Compared with acceleration response, strain measurement is more sensitive to structural local or minor damages. Thus, objective function *Obj*2 established based on combined correlation function of strain response is employed to identify small damages. In damage case 3, assuming 10% and 6% stiffness are reduced in elements 6 and 13, respectively, namely $\alpha_6 = 0.1$, $\alpha_{13} = 0.06$. Two strain gauges at elements 4, 10, and eight strain gauges at elements 2, 4, 7, 8, 10, 12, 14, 16, are adopted to consider the effect of the number of sensors, and their damage identification results using *Obj*2 are provided in Fig. 7. Several false identifications are obviously observed at elements 6, 12, and 13 with two sensors. On the contrary, pleasant results are obtained with average error of 0.81% and maximum error of 2.41% under 20% noise, as listed in Table 2, when installed eight strain gauges on the structure, which demonstrates that combined strain correlation function-based objective function *Obj*2 is able to accurately identify relatively small damages but requires more sensors for the reason that strain gauges can only reflect the point-to-point local information near the sensor's proximity.

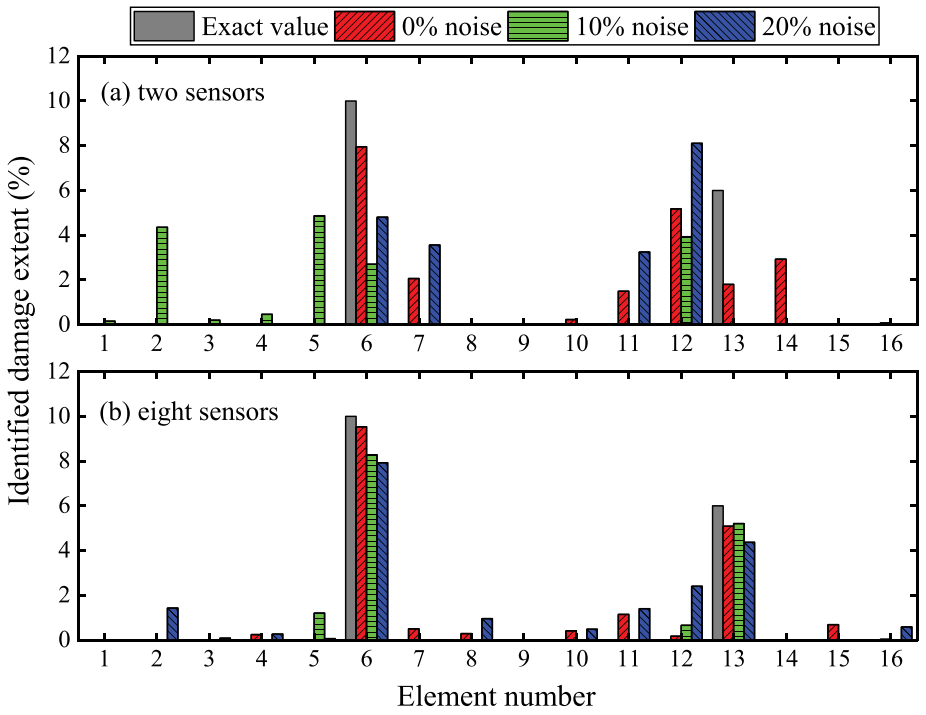


**Figure 7:** Identified damage results with *Obj*2 in case 3: (**a**) two sensors; (**b**) eight sensors

**Table 2:** Identified results based on four different objective functions (%)

| Cases | Objective functions | Noise free | | 10% noise | | 20% noise | |
|---|---|---|---|---|---|---|---|
| | | Mean error | Max error | Mean error | Max error | Mean error | Max error |
| Case1 | *Obj*1 | 0.66 | 2.54 | 1.13 | 5.82 | 1.75 | 7.69 |
| Case2 | *Obj*1 | 1.86 | 9.14 | 4.07 | 12.96 | 3.75 | 13.73 |
| Case3 | *Obj*2-2 sensors | 1.25 | 5.18 | 2.03 | 7.29 | 2.01 | 8.11 |
| | *Obj*2-8 sensors | 0.35 | 1.15 | 0.36 | 1.72 | 0.81 | 2.41 |
| Case4 | *Obj*3 | 0.34 | 2.14 | 0.88 | 3.56 | 1.05 | 3.93 |
| | *Obj*4 | 0.15 | 0.87 | 0.37 | 1.49 | 0.42 | 1.56 |

To evaluate the effectiveness of the proposed hybrid objective functions *Obj*3 and *Obj*4, a comprehensive case study, denoted as case 4, is conducted. This study examines the identification performance under both severe and minor damage conditions to ensure the method's versatility. Assuming 20%, 10% and 6% stiffness are reduced in elements 6, 10 and 13, namely $\alpha_6 = 0.2$, $\alpha_{10} = 0.1$, $\alpha_{13} = 0.06$. To closely mimic actual engineering practice, two accelerometers and two strain gauges are placed to capture both dynamic and local strain responses. The regularization parameter $\lambda$ is set as $1 \times 10^{-4}$. Identified damage results using *Obj*3 and *Obj*4 are shown in Fig. 8 and Table 2. When *Obj*3 is applied, the identification accuracy remains acceptable even under 20% noise, with the maximum error of estimated parameters below 4%. However, several intact elements, such as 4, 5, 9, 11, and 15, are mistakenly identified as damaged, indicating its limited robustness against noise. In contrast, *Obj*4, enhanced with sparse regularization, yields significantly improved results. The average

error decreases to 0.42% and the maximum error is reduced to 1.56%, with nearly no false identifications. These results confirm that introducing sparsity not only enhances numerical stability but also ensures reliable discrimination between real and spurious damage, thereby providing a more robust framework for practical structural damage detection.

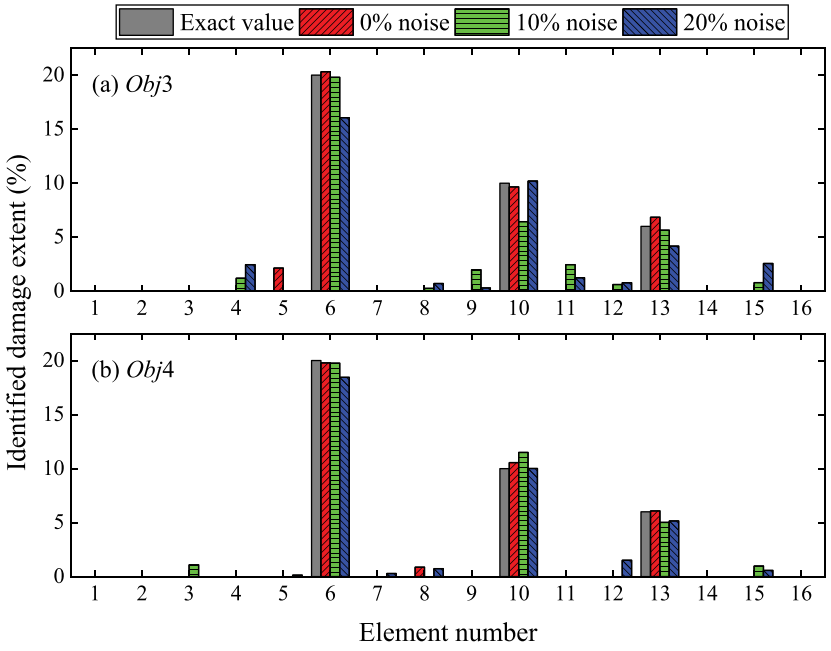


**Figure 8:** Identified damage results with the proposed hybrid objective function: (**a**) *Obj*3; (**b**) *Obj*4

### *5.2 Comparison with Other Optimization Algorithms*

The effectiveness and advantages of the proposed MHSO algorithm are further evaluated in damage case 5 through a comparative study involving three widely used optimization methods. The adopted parameters of sequential quadratic programming (SQP), GA, HSO and MHSO are listed in Table 3. Stiffness reductions of 8% and 15% are introduced in elements 6 and 13, corresponding to damage indices of $\alpha_6 = 0.08$, $\alpha_{13} = 0.15$ to simulate both minor and moderate damage scenarios. The monitoring arrangements are two accelerometers positioned at nodes 5 and 10, along with two strain gauges placed at the midpoints of elements 8 and 14, thereby capturing both dynamic and local strain responses. The hybrid objective function *Obj*4 is adopted for damage identification, with a regularization parameter set to $\lambda = 1 \times 10^{-4}$, enabling the effective balancing of accuracy and sparsity. This comparative analysis is designed to highlight the superior performance of the MHSO algorithm in terms of damage localization accuracy, robustness under noise contamination, and convergence efficiency, thereby demonstrating its significant potential for practical structural health monitoring applications.

**Table 3:** Parameters of SQP, GA, HSO, MHSO

| Parameters | SQP | GA [49] | HSO | MHSO |
|---|---|---|---|---|
| Initial value | $0.8 \times \theta_{act}$ | | | |
| Population size *NP* | | 100 | 100 | 100 |
| Maximum iterations $G_m$ | | 400 | 200 | 100 |

(Continued)

**Table 3 (continued)**

| Parameters | SQP | GA [49] | HSO | MHSO |
|---|---|---|---|---|
| Mutation probability | | 0.2 | | |
| Crossover probability | | 0.8 | | |

A comparative analysis of damage identification performance using SQP, GA, HSO, and the proposed MHSO algorithm under different noise conditions (0%, 10%, and 20%) is presented to evaluate their robustness and accuracy. As presented in Fig. 9 and Table 4, SQP and GA, representing gradient-based and classical heuristic optimization approaches, exhibit significant degradation in accuracy when noise levels increase. In particular, both methods fail to reliably detect minor stiffness reductions, under moderate and high noise contamination. The HSO algorithm, as a modern swarm intelligence technique, demonstrates better robustness to noise and is able to locate damaged elements; however, it encounters difficulties in precisely quantifying damage severity, resulting in noticeable estimation errors. In contrast, the proposed MHSO algorithm achieves consistently high accuracy across all noise levels. Even under the harsh condition of 20% noise contamination, MHSO maintains superior performance with minimal error, effectively identifying both damage location and magnitude. In addition, the statistical results of SQP, GA, HSO and MHSO under 0% noise are listed in Table 5. It is evident that the proposed MHSO achieves the smallest mean error and standard deviation, indicating its strong stability and high reliability in damage identification performance. The comparative results clearly highlight the advantages of MHSO in both stability and precision over traditional and existing optimization approaches. Fig. 10 illustrates the iterative convergence process of the MHSO algorithm, showing that identified damage parameters steadily approach the true values. Notably, convergence is achieved within approximately 80 iterations, demonstrating the algorithm's high efficiency. These results clearly highlight the robustness, precision, and rapid convergence capability of the proposed MHSO approach.

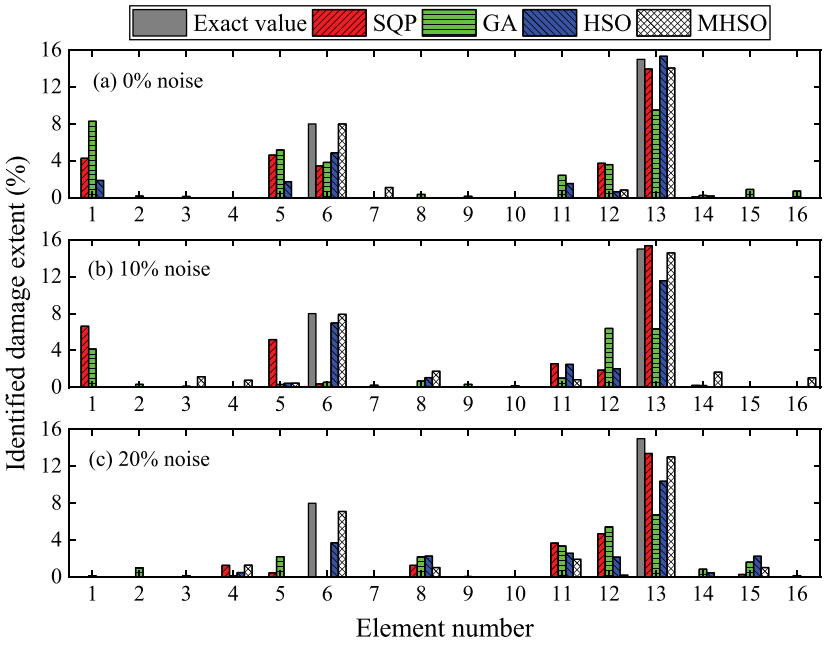


**Figure 9:** Identification results for SQP, GA, HSO, MHSO: (**a**) 0% noise; (**b**) 10% noise; (**c**) 20% noise

**Table 4:** Identified mean and maximum errors under three levels of noise (%)

| Methods | 0% noise | | 10% noise | | 20% noise | |
|---|---|---|---|---|---|---|
| | Mean error | Max error | Mean error | Max error | Mean error | Max error |
| SQP | 1.35 | 4.62 | 1.89 | 7.63 | 1.72 | 8.00 |
| GA | 2.36 | 8.28 | 2.28 | 8.67 | 2.46 | 8.27 |
| HSO | 0.74 | 3.14 | 0.82 | 3.45 | 1.39 | 4.61 |
| MHSO | 0.23 | 1.09 | 0.58 | 1.73 | 0.60 | 1.98 |

**Table 5:** The statistical results of the identified elemental damage

| Element | SQP | | GA | | HSO | | MHSO | |
|---|---|---|---|---|---|---|---|---|
| | Mean Value | Std. | Mean Value | Std. | Mean Value | Std. | Mean Value | Std. |
| $\alpha_6$ = 0.08 | 0.0344 | 0.042 | 0.0382 | 0.030 | 0.0486 | 0.024 | 0.0799 | 9.21E−04 |
| $\alpha_{13}$ = 0.15 | 0.1395 | 0.030 | 0.0950 | 0.035 | 0.1533 | 0.011 | 0.1406 | 4.71E−05 |

Note: std. denotes the standard deviation.

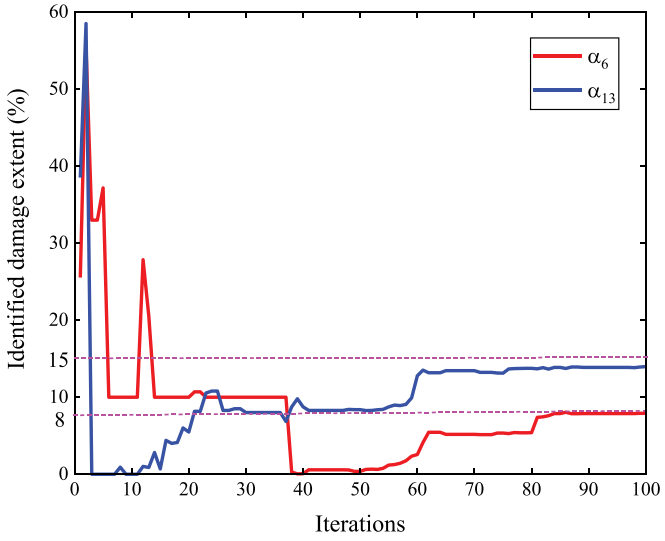


**Figure 10:** The evolutionary process of the identified damage elements with the proposed MHSO

In addition to the identification accuracy, the computational efficiency for SQP, GA, HSO, MHSO is also investigated, listed in Table 6. SQP has the fastest computational speed due to its gradient-based search characteristic. Compared with 2012, 608 and 311 s consumed by GA, HSO, MHSO, only 226 s is needed for SQP, but a good initial guess has to be given. Otherwise, the identified solution is probably trapped into local optimum. Taking the computational time and damage identification accuracy into consideration, the proposed MHSO can achieve better performance than SQP, GA, HSO.

**Table 6:** Comparison of computational time for SQP, GA, HSO, MHSO

| Methods | Number of iterations | Computational time for single iteration (s) | Computational time (s) |
|---|---|---|---|
| SQP | 88 | 2.56 | 226 |
| GA | 400 | 5.03 | 2012 |
| HSO | 200 | 3.04 | 608 |
| MHSO | 100 | 3.11 | 311 |

## 6 Validation with a UCF Benchmark Structure

### *6.1 Finite Element Model*

Further investigations are carried out on a steel grid benchmark structure [50] to comprehensively validate the effectiveness of the proposed damage identification strategy. The experimental tests were conducted at the University of Central Florida, as illustrated in Fig. 11a. The benchmark grid structure has an overall length of 5.49 m and a width of 1.83 m, representing a realistic structural system for validation purposes. A finite element model of the structure is developed, consisting of 19 beam elements interconnected at 14 nodes to accurately simulate its dynamic characteristics. For the boundary condition, columns provide a pinned support for the grid. The elastic modulus and density of steel materials are $2.1 \times 10^{11}$ N/m$^2$ and 7850 kg/m$^3$, respectively. The UCF steel gird benchmark structure was excited by a white noise excitation at node 3. Three accelerometers are installed at nodes 2, 7, 11, to captured the accelerations in vertical direction. Five strain gauges are placed at the midpoint of elements 4, 9, 11, 14, 18 to measure the strain responses. The total duration and sampling rate are of 1800 s and 400 samples/s. More detailed description about the steel gird benchmark structure can be found in Ref. [51].

### *6.2 Damage Identification Results*

As shown in Fig. 12, two damage cases, including large elemental damages and small elemental damages, are considered to verify the effectiveness of the proposed approach. In damage case 1, 20% and 15% stiffness are reduced in elements 15 and 18, respectively, namely $\alpha_{15} = 0.2$, $\alpha_{18} = 0.15$. In damage case 2, 10% and 8% stiffness are reduced in elements 10 and 17, respectively, namely $\alpha_{10} = 0.1$, $\alpha_{17} = 0.08$. Only MHSO algorithm is used owing to its pleasant performance. Population size and maximum iterations are set as 100 and 200. The identified results of damage case 1 and case 2 using MHSO algorithm and hybrid objective functions *Obj*4 are presented in Fig. 12. For case 1, the identified values are $\alpha_{15} = 0.1942$, $\alpha_{18} = 0.1531$, very close to the exact values. Mean error and maximum error listed in Table 7 are 0.66% and 2.92%. For case 2, the identified values are $\alpha_{10} = 0.1017$, $\alpha_{17} = 0.0767$, corresponding to 1.67% and 1.66% small relative errors. The results demonstrate that the proposed output-only damage identification method, which integrates the MHSO algorithm with a hybrid objective function based on combined acceleration function and strain correlation function, is capable of accurately detecting both significant and subtle structural damages, offering a promising solution for efficient and reliable damage detection in complex structural systems.

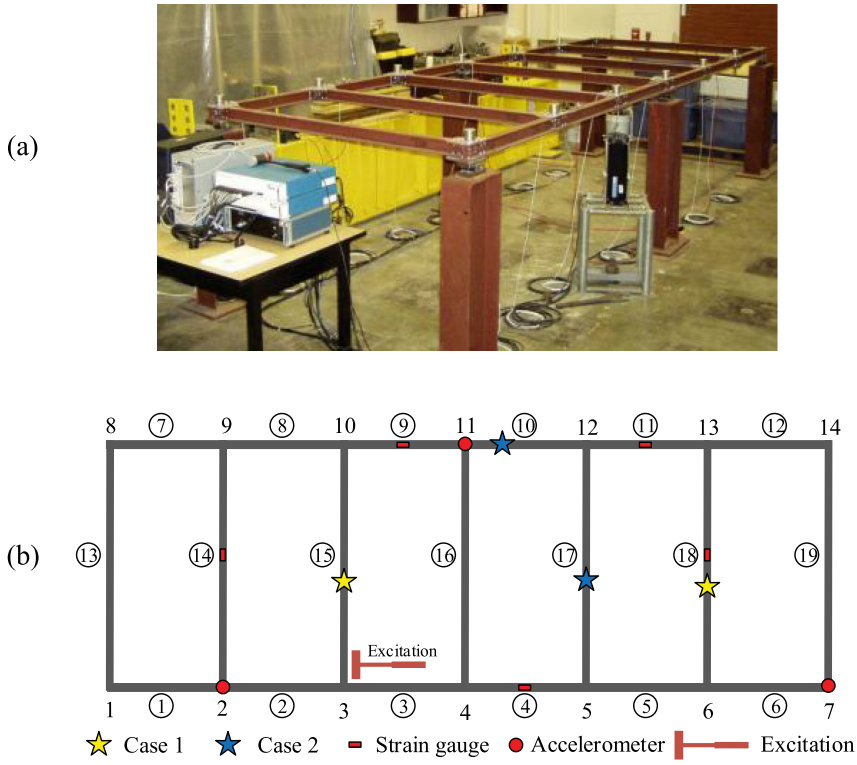


**Figure 11:** Steel gird benchmark structure: (**a**) experimental model; (**b**) setup of sensors and damage cases

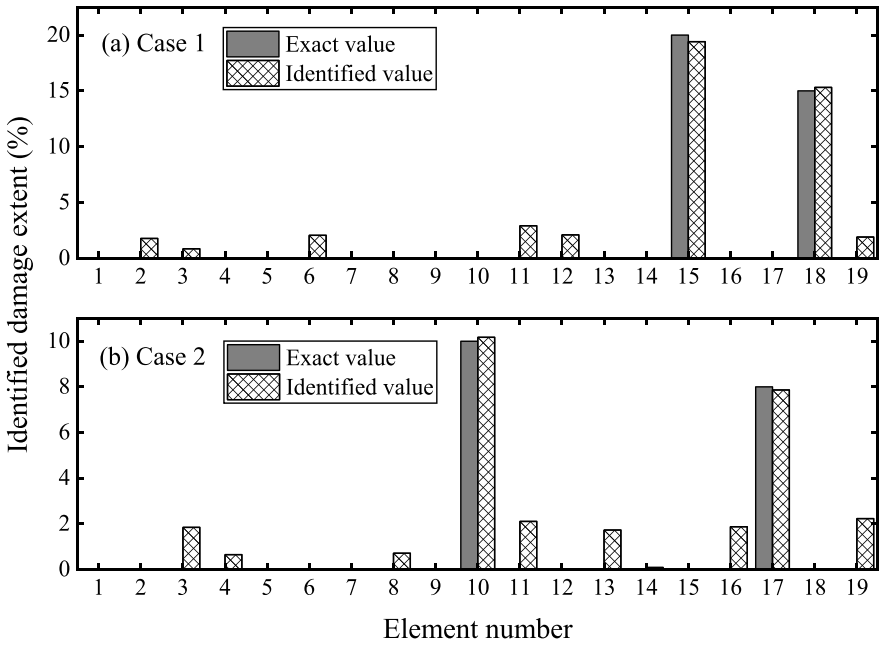


**Figure 12:** Damage identification results for steel gird benchmark structure: (**a**) case 1; (**b**) case 2

**Table 7:** The identified values and errors for steel gird benchmark structure

| Damage cases | Damage element | | Error (%) | |
|---|---|---|---|---|
| | Identified values | Relative error (%) | Mean error | Maximum error |
| Case 1 | $\alpha_{15}$ = 0.1942<br>$\alpha_{18}$ = 0.1531 | 2.92<br>2.09 | 0.66 | 2.92 |
| Case 2 | $\alpha_{10}$ = 0.1017<br>$\alpha_{17}$ = 0.0767 | 1.67<br>1.66 | 0.61 | 2.23 |

## 7 Discussions

### *7.1 Robustness to Non-Gaussian Noise*

To comprehensively evaluate the robustness and stability of the proposed approach, additional numerical simulations are conducted under non-Gaussian noise conditions, including impulsive noise and outliers, which commonly occur in real-world monitoring. Unlike Gaussian noise, which affects all measurements uniformly, impulsive noise and outliers introduce sporadic, large-magnitude disturbances that can significantly distort the measured responses and challenge the identification process. The proposed MHSO algorithm with $L_{0.5}$ sparse regularization is applied to these noise-contaminated measurements to assess its resilience in maintaining accurate and stable damage identification. The damage case 4 of the 16-element simply-supported beam structure is utilized as numerical example. Results show that the method exhibits strong robustness against impulsive interference, effectively distinguishing structural response patterns from abnormal measurement. Even when up to 10% of the measurements were corrupted by impulsive outliers, the algorithm accurately localized the damaged elements. This performance can be attributed to the inherent sparsity-promoting and outlier-suppressing capability of the $L_{0.5}$ sparse regularization, which adaptively reduces the influence of non-Gaussian perturbations while preserving essential structural features. These results confirm that the proposed MHSO framework achieves high robustness and stability across diverse noise environments.

### *7.2 Comparative Analysis with Traditional Regularization Methods*

Comparative studies of $L_{0.5}$ sparse regularization method introduced in the paper with traditional $L_1$ and $L_2$ regularization methods are conducted. The damage case 4 of the 16-element simply-supported beam structure is utilized herein. Assuming 20%, 10% and 6% stiffness are reduced in elements 6, 10 and 13, namely $\alpha_6$ = 0.2, $\alpha_{10}$ = 0.1, $\alpha_{13}$ = 0.06. The identified results using MHSO with different regularization methods are shown in Table 8.

**Table 8:** Identified results based on four different objective functions (%)

| Regularization methods | Noise free | | 10% noise | | 20% noise | |
|---|---|---|---|---|---|---|
| | Mean error | Max error | Mean error | Max error | Mean error | Max error |
| $L_1$ | 0.54 | 4.72 | 1.70 | 7.46 | 2.06 | 8.49 |
| $L_2$ | 0.46 | 5.92 | 1.65 | 6.99 | 2.13 | 9.44 |
| $L_{0.5}$ | 0.15 | 0.87 | 0.37 | 1.49 | 0.42 | 1.56 |

Under identical noise conditions (0%, 10%, and 20%). The results show that $L_{0.5}$ achieves the smallest mean error and highest noise robustness. In comparison with conventional $L_1$ and $L_2$ regularizations, the proposed $L_{0.5}$ sparse penalty provides a non-convex approximation to the ideal $L_0$ norm, thus achieving stronger sparsity. Numerical comparisons indicate that while $L_1$ regularization may introduce bias in small-damage estimation and $L_2$ regularization tends to over-smooth the results, $L_{0.5}$ effectively suppresses noise and maintains the true sparsity pattern of damage indices. This advantage becomes particularly evident under high noise contamination or when multiple minor damages coexist. Therefore, $L_{0.5}$ regularization offers a practical balance between computational tractability and physical interpretability for robust damage identification.

### *7.3 Strategies for Improving Computational Efficiency*

Computational efficiency is crucial for practical SHM applications, particularly when dealing with large-scale structures or real-time systems. In the current study, the computational cost of MHSO is moderate due to the lightweight population update mechanism of the holistic swarm framework, which eliminates complex control parameters and gradient evaluations. For large-scale structures with thousands of elements, further acceleration is desirable. To this end, several strategies can be implemented and validated in our future work to extend the applicability of MHSO to large-scale or real-time SHM scenarios.

(1) Parallelization: The evaluation of the objective function for different individuals can be parallelized using multi-core Central Processing Unit (CPUs) or Graphics Processing Unit (GPUs) to significantly reduce computation time.
(2) Surrogate-assisted optimization: Incorporating surrogate models (e.g., radial basis functions or Gaussian processes) can approximate the objective function and reduce the number of finite element evaluations.
(3) Model reduction: The combination of MHSO with reduced-order modeling (e.g., component mode synthesis or substructure) will be explored to further enhance real-time applicability.

### *7.4 Practical Applicability*

Structural health monitoring often involves dealing with environmental variations, temperature changes, and non-linear damage. The adaptability of the proposed method to more realistic conditions will be pursued in future work through the following directions:

(1) Environmental and temperature effects: Incorporate environmental variability compensation techniques (e.g., cointegration analysis or temperature-response decoupling) to reduce false damage indications.
(2) Nonlinear damage modeling: The MHSO framework will be extended to handle nonlinear stiffness degradation or contact-type damages by integrating nonlinear finite element models or hybrid data-model fusion strategies.
(3) Complex large-scale systems: The algorithm will be validated on large-scale numerical and experimental structures (e.g., steel truss bridges or composite girders) to examine scalability and reliability.
(4) Real-time integration: Coupling the proposed approach with edge computing and digital twin platforms will be investigated to enable continuous, online monitoring and rapid damage assessment.

## 8 Conclusions

This study introduces a novel and robust strategy for structural damage identification that integrates a modified holistic swarm optimization algorithm with a hybrid objective function. To overcome the

limitations of the conventional HSO framework, several enhancements are incorporated. First, the population initialization is improved through the application of the Hammersley sequence, which ensures a more uniform distribution of candidate solutions in the search space. Second, a chaotic search strategy is performed around the worst individual to strengthen global exploration ability and avoid premature convergence. Third, a local refinement is conducted using the Hooke–Jeeves pattern search in the vicinity of the best solution, thereby improving the convergence speed and accuracy of the optimization process. The effectiveness of the proposed methodology is validated through two benchmark studies: a simply supported beam model and a steel grid benchmark structure. Validation on a simply supported beam and a steel grid benchmark confirms the reliability of the approach. Conclusions can be summarized as follows:

(1) In terms of computational efficiency and accuracy, MHSO consistently outperforms SQP, GA, and the standard HSO. The improved search mechanism effectively balances exploration and exploitation, resulting in superior convergence behavior.
(2) While acceleration-based correlation functions struggle to detect small-scale damage, and strain-based correlation functions require dense sensor networks, the hybrid formulation successfully addresses both limitations. The introduction of sparse regularization further improves identification accuracy and robustness in noisy environments.
(3) The proposed approach demonstrates the ability to detect both large and small damages with limited sensor deployment, maintaining reliable performance even when the measurements are contaminated with up to 20% Gaussian noise.

Despite its promising performance, several limitations of the proposed approach should be acknowledged. First, the current validation is limited to beam-type and benchmark girder structures. The extension to more complex or large-scale systems may introduce higher-dimensional parameter spaces, which could affect convergence efficiency and computational scalability. Second, although the hybrid optimization strategy accelerates convergence, the combined use of Hammersley initialization, chaotic search, and Hooke–Jeeves refinement inevitably increases computational cost compared with standard metaheuristics. Future work will focus on employing parallel computation and surrogate-assisted optimization to mitigate this issue. Third, while the hybrid objective function reduces sensitivity to sensor configuration, damage detection accuracy still depends on sensor density and placement. Optimization of sensor layout and fusion with additional sensing modalities will be further investigated.

**Acknowledgement:** Not applicable.

**Funding Statement:** The authors received no specific funding for this study.

**Author Contributions:** Xiansong Xie: Writing—Original Draft Preparation, Conceptualization, Methodology, Investigation, Software. Xiaoqian Qian: Supervision, Conceptualization, Writing—Reviewing and Editing. All authors reviewed the results and approved the final version of the manuscript.

**Availability of Data and Materials:** Data available on request from the authors.

**Ethics Approval:** Not applicable.

**Conflicts of Interest:** The authors declare no conflicts of interest to report regarding the present study.

## References

1. Fan W, Qiao P. Vibration-based damage identification methods: a review and comparative study. Struct Health Monit. 2011;10(1):83–111. doi:10.1177/1475921710365419.

2. Avci O, Abdeljaber O, Kiranyaz S, Hussein M, Gabbouj M, Inman DJ. A review of vibration-based damage detection in civil structures: from traditional methods to machine learning and deep learning applications. Mech Syst Signal Process. 2021;147:107077. doi:10.1016/j.ymssp.2020.107077.
3. Su WC, Huang CS, Hung SL, Chen LJ, Lin WJ. Locating damaged storeys in a shear building based on its substructural natural frequencies. Eng Struct. 2012;39(1):126–38. doi:10.1016/j.engstruct.2012.02.002.
4. Katunin A, Huňady R, Hagara M. Damage identification in composite structures using high-speed 3D digital image correlation and wavelet analysis of mode shapes. Nondestruct Test Eval. 2025;40(8):3650–68. doi:10.1080/10589759.2024.2407893.
5. Nguyen KD, Chan TH, Thambiratnam DP, Nguyen A. Damage identification in a complex truss structure using modal characteristics correlation method and sensitivity-weighted search space. Struct Health Monit. 2019;18(1):49–65. doi:10.1177/1475921718809471.
6. Ahmadi-Nedushan B, Fathnejat H. A modified teaching-learning optimization algorithm for structural damage detection using a novel damage index based on modal flexibility and strain energy under environmental variations. Eng Comput. 2022;38(1):847–74. doi:10.1007/s00366-020-01197-3.
7. Ghannadi P, Khatir S, Kourehli SS, Nguyen A, Boutchicha D, Abdel Wahab M. Finite element model updating and damage identification using semi-rigidly connected frame element and optimization procedure: an experimental validation. Structures. 2023;50:1173–90. doi:10.1016/j.istruc.2023.02.008.
8. Perry MJ, Koh CG. Output-only structural identification in time domain: numerical and experimental studies. Earthq Eng Struct Dyn. 2008;37(4):517–33. doi:10.1002/eqe.769.
9. Li Y, Wang S, Tapia J, Xia Z, An W. An iterative total least squares-based estimation method for structural damage identification of 3D frame structures. Struct Control Health Monit. 2020;27(4):e2499. doi:10.1002/stc.2499.
10. Zhang YM, Wang H, Wan HP, Mao JX, Xu YC. Anomaly detection of structural health monitoring data using the maximum likelihood estimation-based Bayesian dynamic linear model. Struct Health Monit. 2021;20(6):2936–52. doi:10.1177/1475921720977020.
11. Zhang C, Huang JZ, Song GQ, Chen L. Structural damage identification by extended Kalman filter with *l*1-norm regularization scheme. Struct Control Health Monit. 2017;24(11):e1999. doi:10.1002/stc.1999.
12. Cadini F, Sbarufatti C, Corbetta M, Giglio M. A particle filter-based model selection algorithm for fatigue damage identification on aeronautical structures. Struct Control Health Monit. 2017;24(11):e2002. doi:10.1002/stc.2002.
13. Li Z, Lin W, Zhang Y. Real-time drive-by bridge damage detection using deep auto-encoder. Structures. 2023;47:1167–81. doi:10.1016/j.istruc.2022.11.094.
14. Li Z, Lan Y, Lin W. Footbridge damage detection using smartphone-recorded responses of micromobility and convolutional neural networks. Autom Constr. 2024;166:105587. doi:10.1016/j.autcon.2024.105587.
15. Ghannadi P, Kourehli SS. Multiverse optimizer for structural damage detection: numerical study and experimental validation. Struct Des Tall Spec Build. 2020;29(13):e1777. doi:10.1002/tal.1777.
16. Tran-Ngoc H, Khatir S, Ho-Khac H, De Roeck G, Bui-Tien T, Abdel Wahab M. Efficient artificial neural networks based on a hybrid metaheuristic optimization algorithm for damage detection in laminated composite structures. Compos Struct. 2021;262:113339. doi:10.1016/j.compstruct.2020.113339.
17. Wang N, Jiang Y, Zhong Y, Shao L. An adaptive damage detection method based on differential evolutionary algorithm for beam structures. Measurement. 2021;178:109227. doi:10.1016/j.measurement.2021.109227.
18. Fatahi L, Moradi S. Multiple crack identification in frame structures using a hybrid Bayesian model class selection and swarm-based optimization methods. Struct Health Monit. 2018;17(1):39–58. doi:10.1177/1475921716683360.
19. Ding Z, Li J, Hao H, Lu ZR. Structural damage identification with uncertain modelling error and measurement noise by clustering based tree seeds algorithm. Eng Struct. 2019;185:301–14. doi:10.1016/j.engstruct.2019.01.118.
20. Yi TH, Li HN, Song G, Zhang XD. Optimal sensor placement for health monitoring of high-rise structure using adaptive monkey algorithm. Struct Control Health Monit. 2015;22(4):667–81. doi:10.1002/stc.1708.
21. Li W, Zou B, Luo Y, Yang N, Zhang F, Jiang M, et al. Impact damage identification of aluminum alloy reinforced plate based on GWO-ELM algorithm. Struct Durab Health Monit. 2023;17(6):485–500. doi:10.32604/sdhm.2023.025989.

22. Luan TM, Khatir S, Tran MT, De Baets B, Cuong-Le T. Exponential-trigonometric optimization algorithm for solving complicated engineering problems. Comput Meth Appl Mech Eng. 2024;432(4):117411. doi:10.1016/j.cma.2024.117411.
23. Li Y, Minh HL, Cao M, Qian X, Abdel Wahab M. An integrated surrogate model-driven and improved termite life cycle optimizer for damage identification in dams. Mech Syst Signal Process. 2024;208:110986. doi:10.1016/j.ymssp.2023.110986.
24. Ghannadi P, Kourehli SS. Efficiency of the slime mold algorithm for damage detection of large-scale structures. Struct Des Tall Spec Build. 2022;31(14):e1967. doi:10.1002/tal.1967.
25. Zhou H, Zhang G, Wang X, Ni P, Zhang J. Structural identification using improved butterfly optimization algorithm with adaptive sampling test and search space reduction method. Structures. 2021;33:2121–39. doi:10.1016/j.istruc.2021.05.043.
26. Xu J, Liu X, Han Q, Wang W. A particle swarm optimization-support vector machine hybrid system with acoustic emission on damage degree judgment of carbon fiber reinforced polymer cables. Struct Health Monit. 2021;20(4):1551–62. doi:10.1177/1475921720922824.
27. Akbari E, Rahimnejad A, Gadsden SA. Holistic swarm optimization: a novel metaphor-less algorithm guided by whole population information for addressing exploration-exploitation dilemma. Comput Meth Appl Mech Eng. 2025;445:118208. doi:10.1016/j.cma.2025.118208.
28. Venkata Rao R. Jaya: a simple and new optimization algorithm for solving constrained and unconstrained optimization problems. Int J Indust Eng Computat. 2016;7(1):19–34. doi:10.5267/j.ijiec.2015.8.004.
29. Rao RV. Rao algorithms: three metaphor-less simple algorithms for solving optimization problems. Int J Indust Eng Computat. 2020;11(1):107–30. doi:10.5267/j.ijiec.2019.6.002.
30. Ni P, Xia Y, Law SS, Zhu S. Structural damage detection using auto/cross-correlation functions under multiple unknown excitations. Int J Str Stab Dyn. 2014;14(5):1440006. doi:10.1142/s0219455414400069.
31. Wang X, Zhang G, Wang X, Ni P. Output-only structural parameter identification with evolutionary algorithms and correlation functions. Smart Mater Struct. 2020;29(3):035018. doi:10.1088/1361-665x/ab6ce9.
32. Zhang G, Wan C, Xiong X, Xie L, Noori M, Xue S. Output-only structural damage identification using hybrid Jaya and differential evolution algorithm with reference-free correlation functions. Measurement. 2022;199(1):111591. doi:10.1016/j.measurement.2022.111591.
33. Wang S, Ren Q. Relationship between local damage and structural dynamic behavior. Sci China Technol Sci. 2012;55(12):3257–62. doi:10.1007/s11431-012-5032-1.
34. Li XY, Wang LX, Law SS, Nie ZH. Covariance of dynamic strain responses for structural damage detection. Mech Syst Signal Process. 2017;95:90–105. doi:10.1016/j.ymssp.2017.03.020.
35. Li M, Ren WX, Huang TL, Wang NB. Experimental investigations on the cross-correlation function amplitude vector of the dynamic strain under varying environmental temperature for structural damage detection. J Low Freq Noise Vib Act Control. 2020;39(3):631–49. doi:10.1177/1461348418820237.
36. Moaveni B, He X, Conte JP, De Callafon RA. Damage identification of a composite beam using finite element model updating. Comput Aided Civ Infrastruct Eng. 2008;23(5):339–59. doi:10.1111/j.1467-8667.2008.00542.x.
37. Hasni H, Jiao P, Alavi AH, Lajnef N, Masri SF. Structural health monitoring of steel frames using a network of self-powered strain and acceleration sensors: a numerical study. Autom Constr. 2018;85(1):344–57. doi:10.1016/j.autcon.2017.10.022.
38. Davis NT, Sanayei M. Foundation identification using dynamic strain and acceleration measurements. Eng Struct. 2020;208:109811. doi:10.1016/j.engstruct.2019.109811.
39. Álvarez-Briceño R, de Oliveira LPR. Combining strain and acceleration measurements for random force estimation via Kalman filtering on a cantilevered structure. J Sound Vib. 2020;469(1):115112. doi:10.1016/j.jsv.2019.115112.
40. Zhu S, Chen Z, Cai Q, Lei Y, Chen B. Locate damage in long-span bridges based on stress influence lines and information fusion technique. Adv Struct Eng. 2014;17(8):1089–102. doi:10.1260/1369-4332.17.8.1089.
41. Ding Z, Li J, Hao H. Non-probabilistic method to consider uncertainties in structural damage identification based on hybrid Jaya and tree seeds algorithm. Eng Struct. 2020;220(1):110925. doi:10.1016/j.engstruct.2020.110925.

42. Mazzotti M, Mao Q, Bartoli I, Livadiotis S. A multiplicative regularized Gauss-Newton method with trust region Sequential Quadratic Programming for structural model updating. Mech Syst Signal Process. 2019;131:417–33. doi:10.1016/j.ymssp.2019.05.062.
43. Chen Z, Wang Y, Wang H, Liu S, Chan THT. Damage identification in bridge structures based on a novel whale-sand cat swarm optimization algorithm and an improved objective function. Struct Control Health Monit. 2025;2025(1):5587918. doi:10.1155/stc/5587918.
44. Ding Z, Hou R, Xia Y. Structural damage identification considering uncertainties based on a Jaya algorithm with a local pattern search strategy and $L_{0.5}$ sparse regularization. Eng Struct. 2022;261:114312. doi:10.1016/j.engstruct.2022.114312.
45. Zhang G, Wan C, Yang Z, Xie L, Xue S. Damage detection of civil structures based on hybrid optimization algorithm and combined correlation function of heterogeneous responses. Measurement. 2025;246:116678. doi:10.1016/j.measurement.2025.116678.
46. Chen H, Yang C, Deng K, Zhou N, Wu H. Multi-objective optimization of the hybrid wind/solar/fuel cell distributed generation system using Hammersley Sequence Sampling. Int J Hydrogen Energy. 2017;42(12):7836–46. doi:10.1016/j.ijhydene.2017.01.202.
47. Li C, Luo G, Qin K, Li C. An image encryption scheme based on chaotic tent map. Nonlinear Dyn. 2017;87(1):127–33. doi:10.1007/s11071-016-3030-8.
48. Khambampati AK, Ijaz UZ, Lee JS, Kim S, Kim KY. Phase boundary estimation in electrical impedance tomography using the Hooke and Jeeves pattern search method. Meas Sci Technol. 2010;21(3):035501. doi:10.1088/0957-0233/21/3/035501.
49. Zhang Z, Koh CG, Duan WH. Uniformly sampled genetic algorithm with gradient search for structural identification—part II: local search. Comput Struct. 2010;88(19–20):1149–61. doi:10.1016/j.compstruc.2010.07.004.
50. Sanayei M, Khaloo A, Gul M, Necati Catbas F. Automated finite element model updating of a scale bridge model using measured static and modal test data. Eng Struct. 2015;102:66–79. doi:10.1016/j.engstruct.2015.07.029.
51. Catbas FN, Gul M, Burkett JL. Damage assessment using flexibility and flexibility-based curvature for structural health monitoring. Smart Mater Struct. 2008;17(1):015024. doi:10.1088/0964-1726/17/01/015024.